Low- and intermediate-temperature ammonia/hydrogen oxidation in a flow reactor: experiments and a wide-range kinetic modeling

Alessandro Stagni[*1], Suphaporn Arunthanayothin[2], Mathilde Dehue[2], Olivier Herbinet[2], Frédérique Battin-Leclerc[2], Pierre Bréquigny[3], Christine Mounaïm-Rousselle[3], Tiziano Faravelli[1]

[1]*Department of Chemistry, Materials, and Chemical Engineering "G. Natta", Politecnico di Milano, Milano 20133, Italy*

[2]*Laboratoire Réactions et Génie des Procédés, CNRS-Université de Lorraine, 1 rue Grandville, 54000 Nancy, France*

[3]*Université Orléans, INSA-CVL, EA 4229 – PRISME, F-45072 Orléans, France*

Corresponding author: Alessandro Stagni; Email address: alessandro.stagni@polimi.it

Supplementary Material

Table of Contents

1 Flow reactor simulations with literature mechanisms

1.1 Stagni et al. [1]

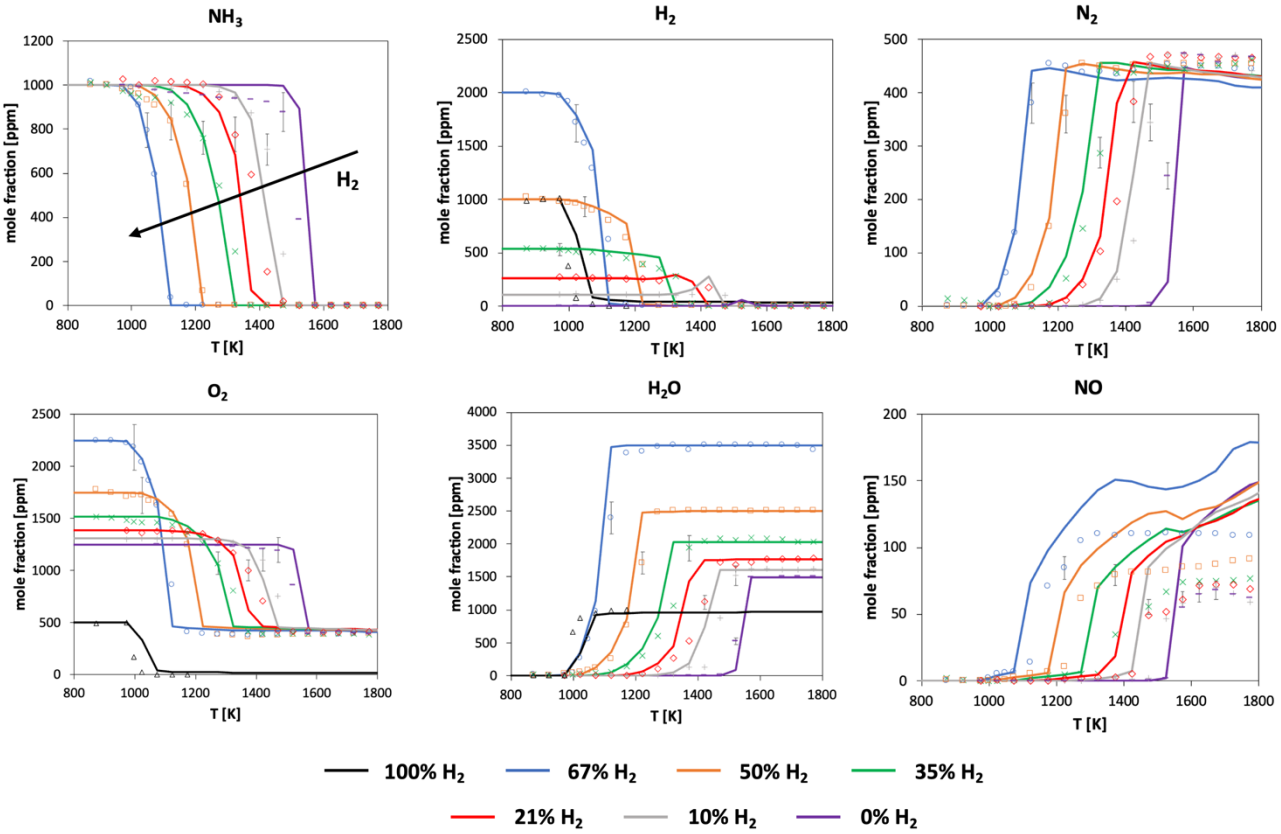

Figure S1. Oxidation of NH_3/H_2 mixture in a flow reactor (cfr Table 1 in the manuscript for the conditions). Experimental and modeling [1] *results.*

1.2 Glarborg et al. [2]

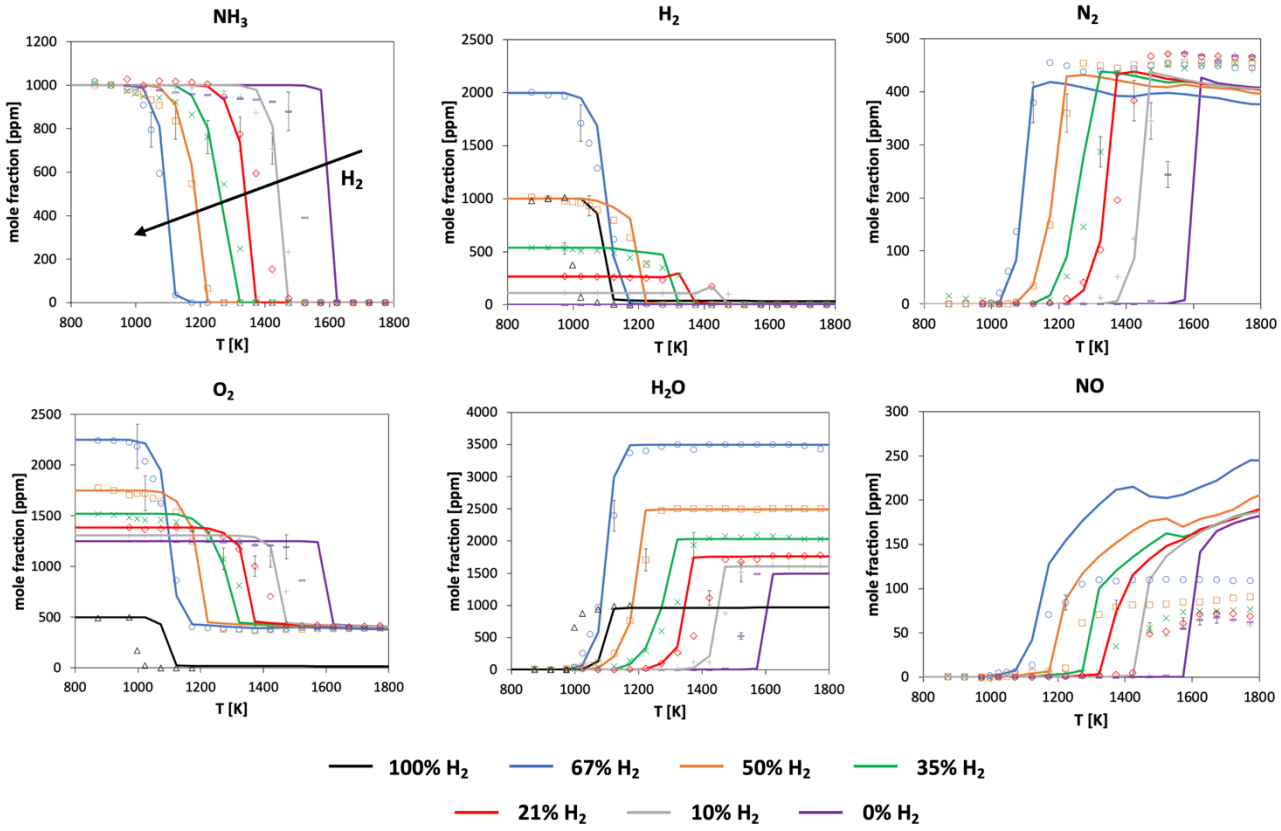

Figure S2. Oxidation of NH_3/H_2 mixture in a flow reactor (cfr Table 1 in the manuscript for the conditions). Experimental and modeling [2] *results.*

1.3 Mei et al. [3]

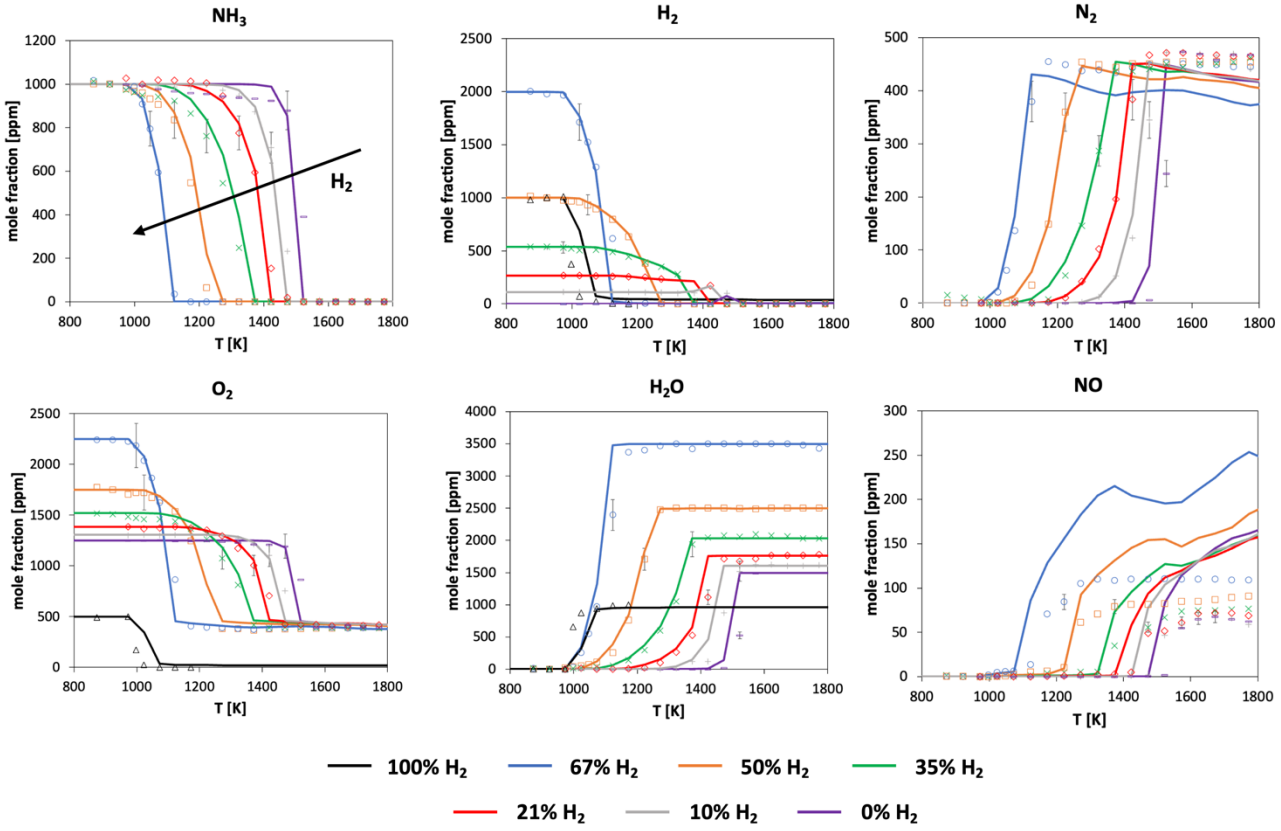

Figure S3. Oxidation of NH_3/H_2 mixture in a flow reactor (cfr Table 1 in the manuscript for the conditions). Experimental and modeling [3] *results.*

1.4 Shrestha et al. [4]

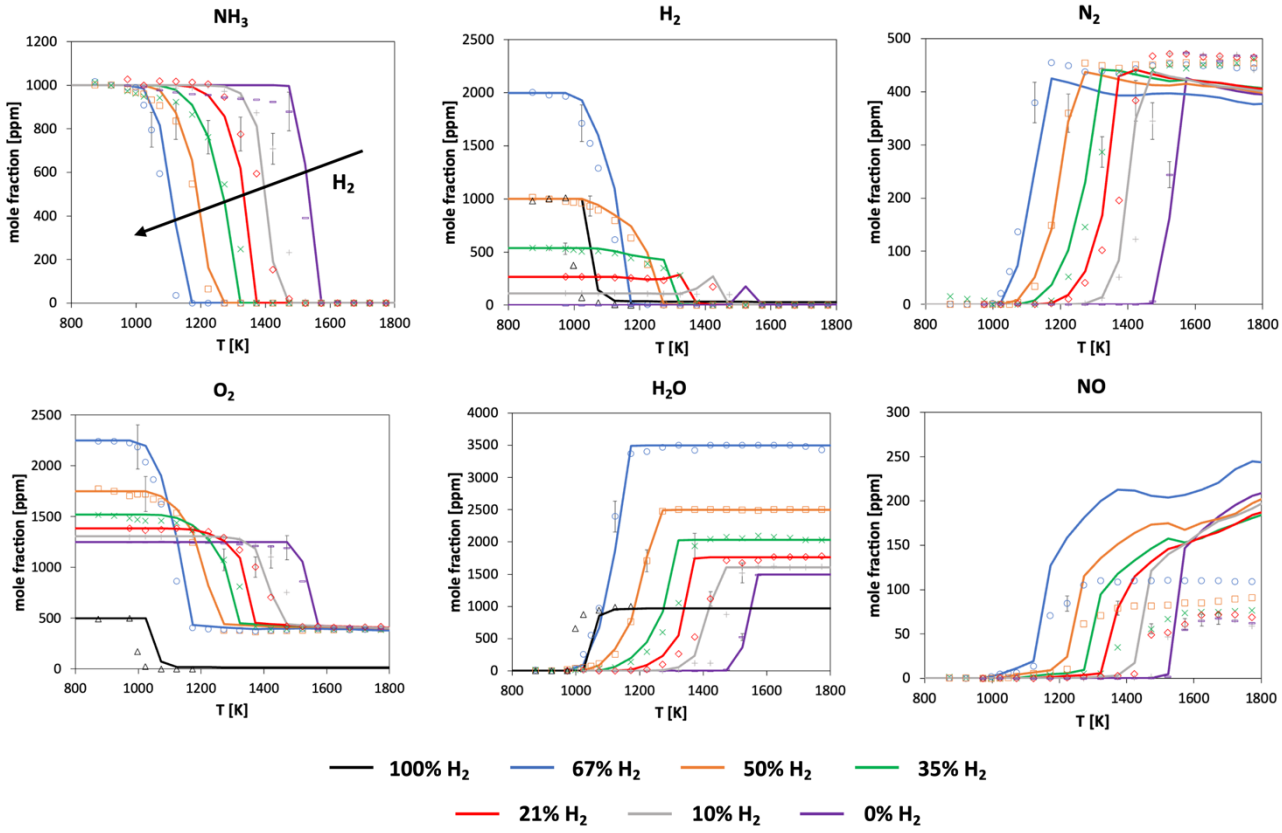

Figure S4. Oxidation of NH_3/H_2 mixture in a flow reactor (cfr Table 1 in the manuscript for the conditions). Experimental and modeling [4] *results.*

1.5 Zhang et al. [5]

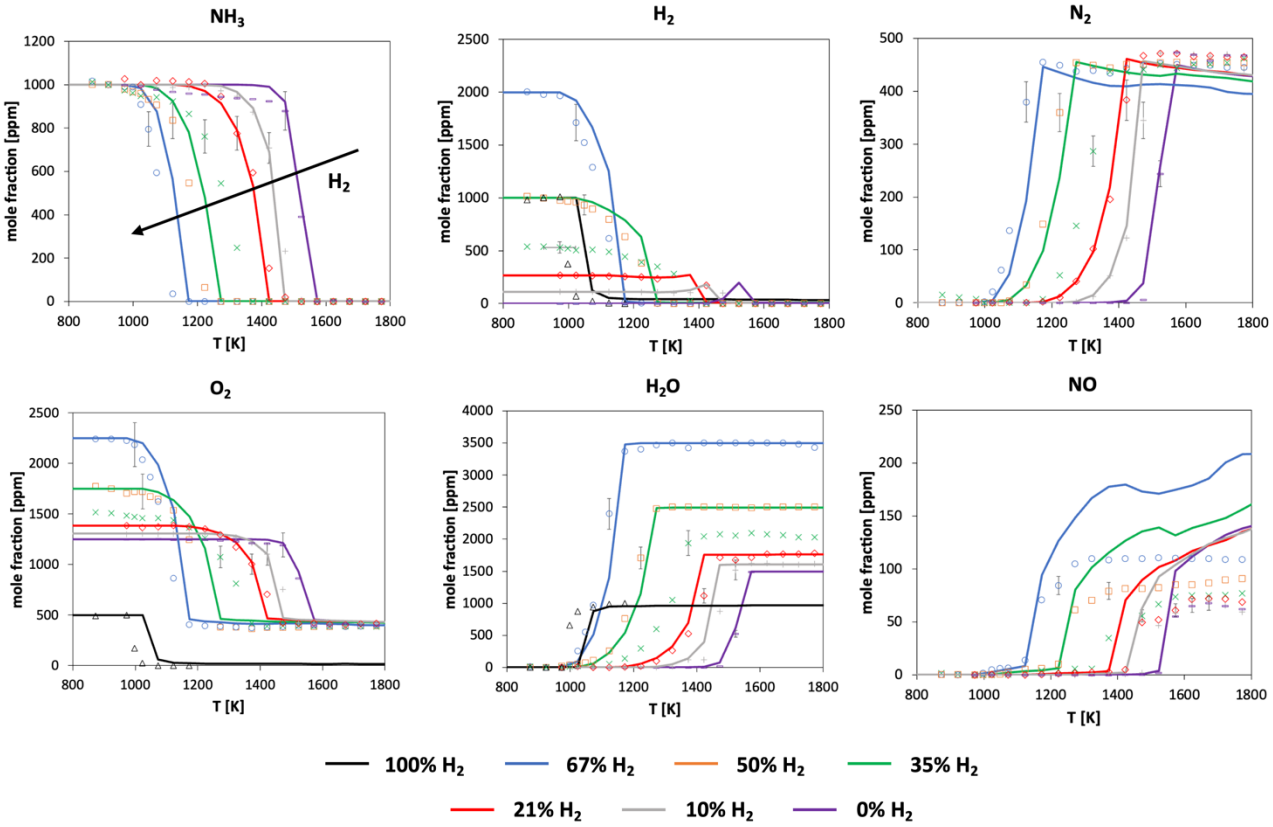

Figure S5. Oxidation of NH_3/H_2 mixture in a flow reactor (cfr. Table 1 in the manuscript for the conditions). Experimental and modeling [5] *results.*

2 Kinetic mechanism validation

2.1 Jet Stirred Reactor

2.1.1 Sabia et al. [6]

Type: Jet Stirred reactor

Model: Non-isothermal Perfectly-Stirred reactor ($U = 1.9 \cdot 10^{-3} \frac{cal}{cm^2 \cdot K \cdot s}$; $A_{exchange} = 113\ cm^2$)

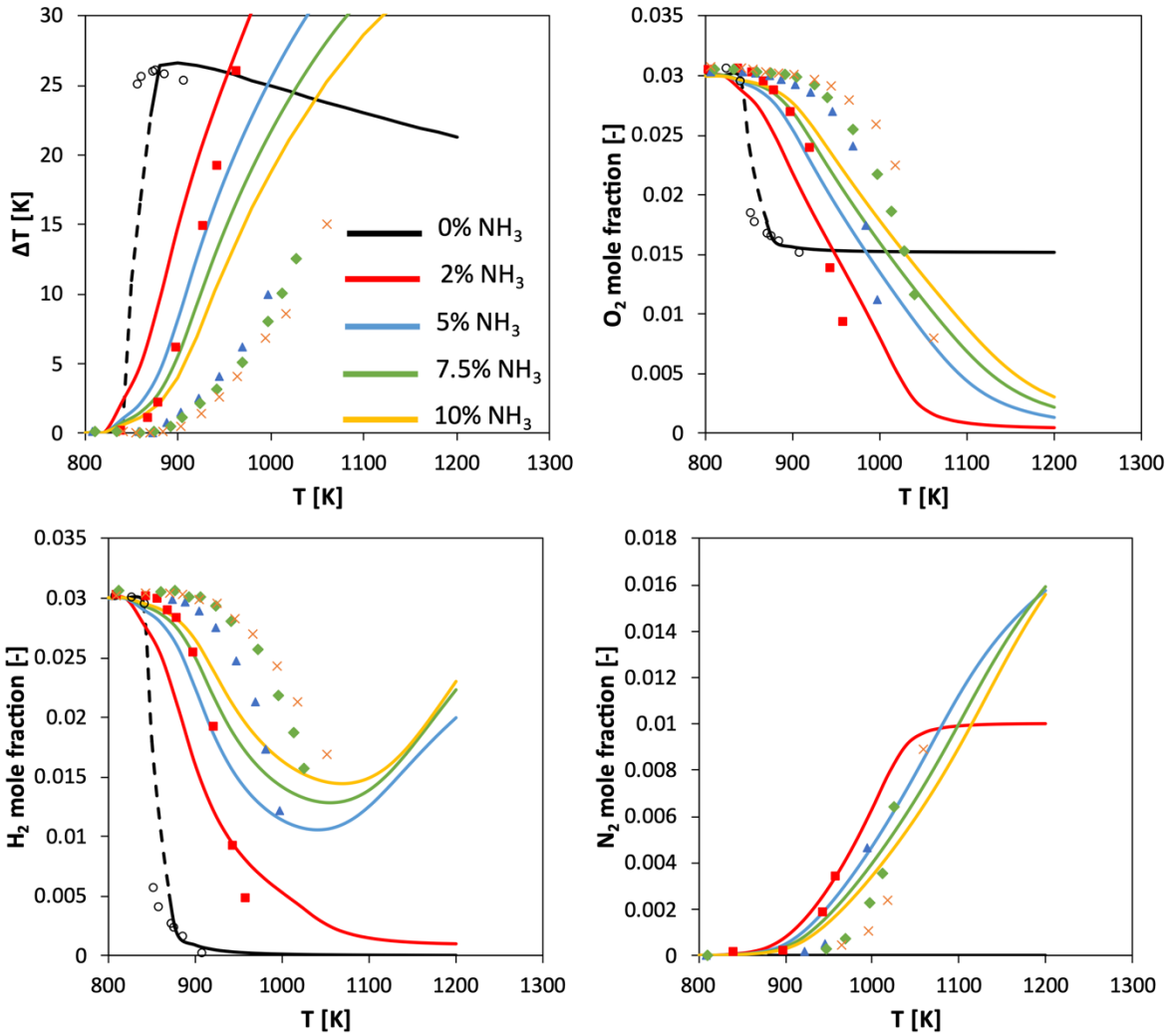

Figure S6. Oxidation of 3% H_2 with 3% O_2 in Ar+NH_3 mixture, with variable NH_3 mole fraction. Φ = 0.5. P = 1.2 atm. Open symbols denote oscillations. Dashed lines indicate average values in the oscillating region. Experimental data [6] *vs modeling results.*

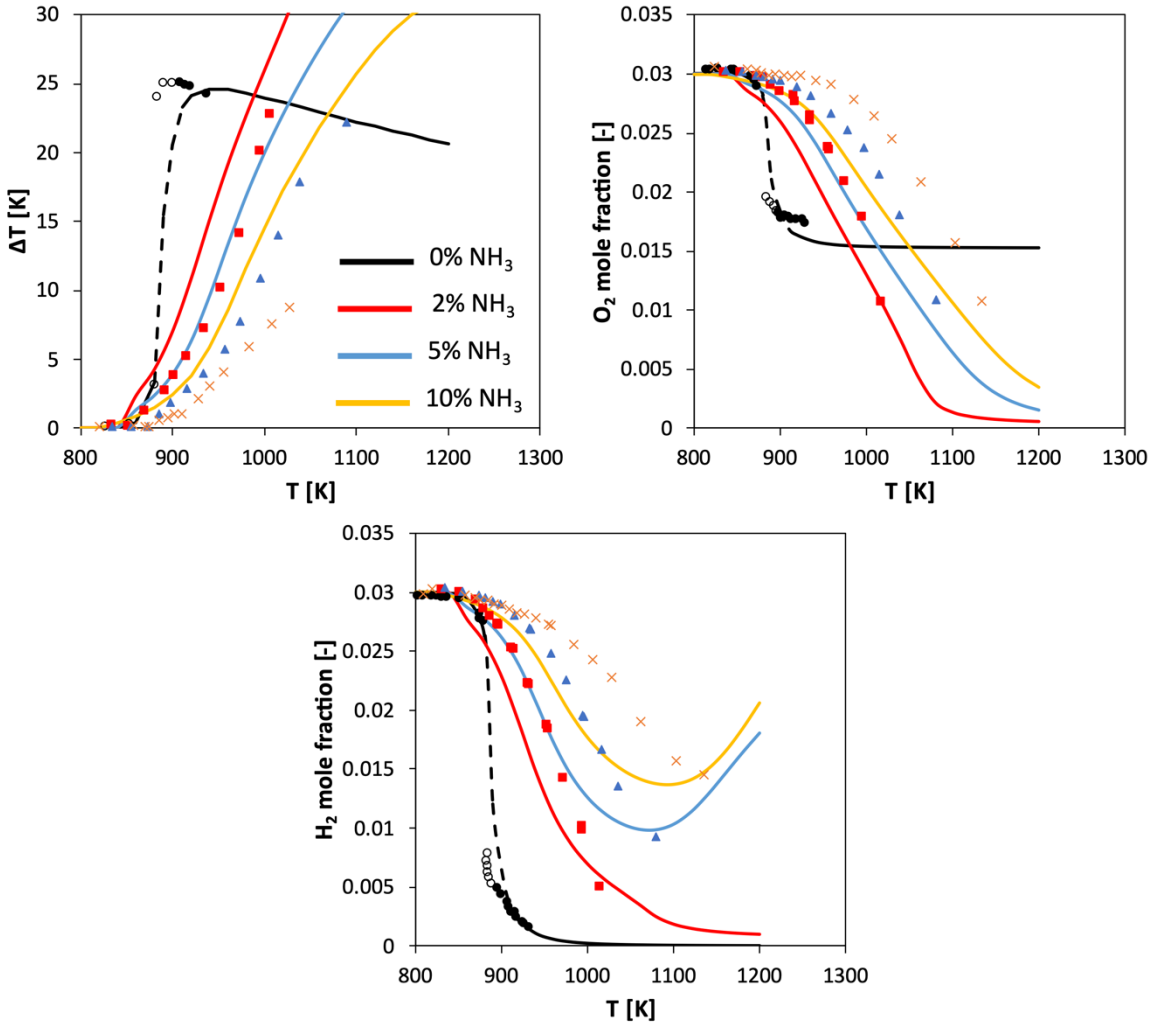

Figure S7. Oxidation of 3% H_2 with 3% O_2 in N_2+NH_3 mixture, with variable NH_3 mole fraction. Φ = 0.5. P = 1.2 atm. Open symbols denote oscillations. Dashed lines indicate average values in the oscillating region. Experimental data [6] *vs modeling results.*

2.1.2 Stagni et al. [1]

Type: Jet Stirred reactor

Model: Isothermal Perfectly-Stirred reactor

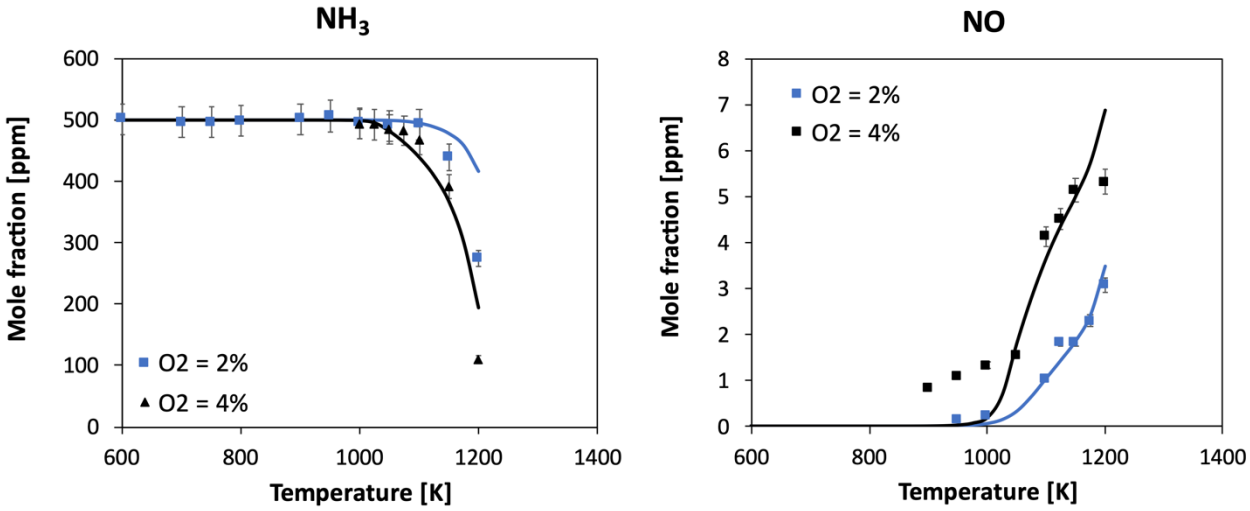

Figure S8. Oxidation of 500 ppm NH_3 in a Jet-Stirred Reactor with 2% and 4% O_2 (mol/mol), respectively. P = 800 torr. τ = 1.5 s. Balance gas: He. Experimental [1] *vs modeling results.*

2.1.3 Zhang et al. [5]

Type: Jet Stirred reactor

Model: Isothermal Perfectly-Stirred reactor

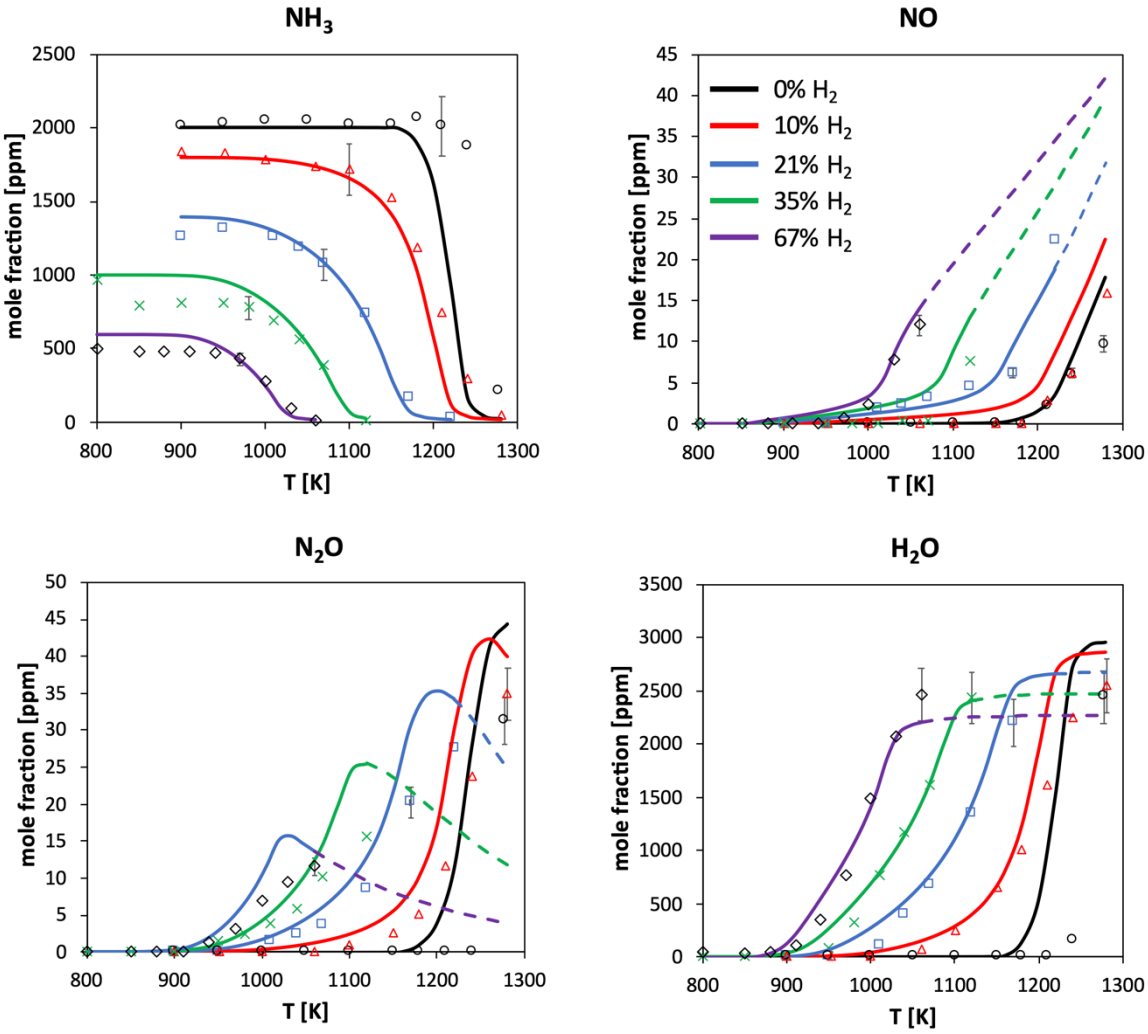

Figure S9. Mole fraction profiles in the oxidation of $NH_3/H_2/O_2/N_2$ mixtures in a JSR. P = 1 atm. Φ = 1 (evaluated with Eq. 1). τ = 1 s. Experimental [5] vs modeling results (dashed lines are predictions outside the experimental range)

2.1.4 Dagaut et al. [7]

Type: Jet Stirred reactor

Model: Isothermal Perfectly-Stirred reactor

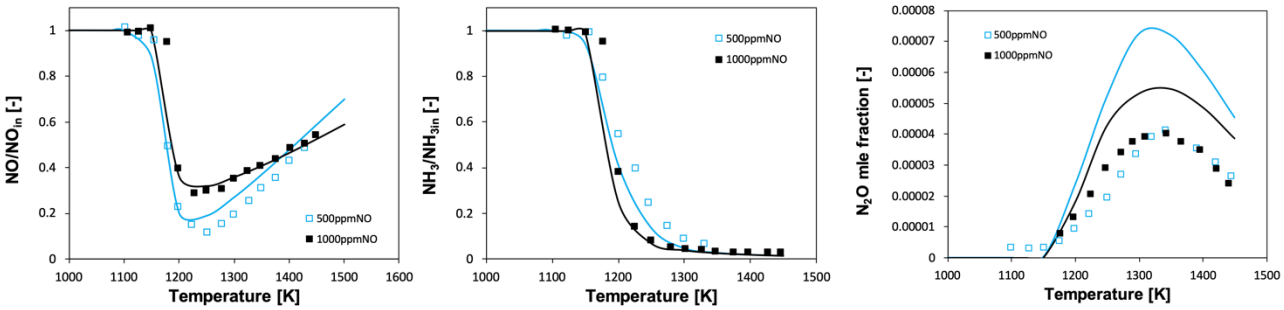

Figure S10. Oxidation of 1000 ppm NH_3 and 12500 ppm O_2 with 500-1000 ppm NO in a Jet Stirred Reactor. Balance gas: N_2. P = 800 torr. τ = 0.1 s. Experimental [7] vs modeling results.

2.1.5 Rota et al. [8]

Type: Jet Stirred reactor

Model: Isothermal Perfectly-Stirred reactor

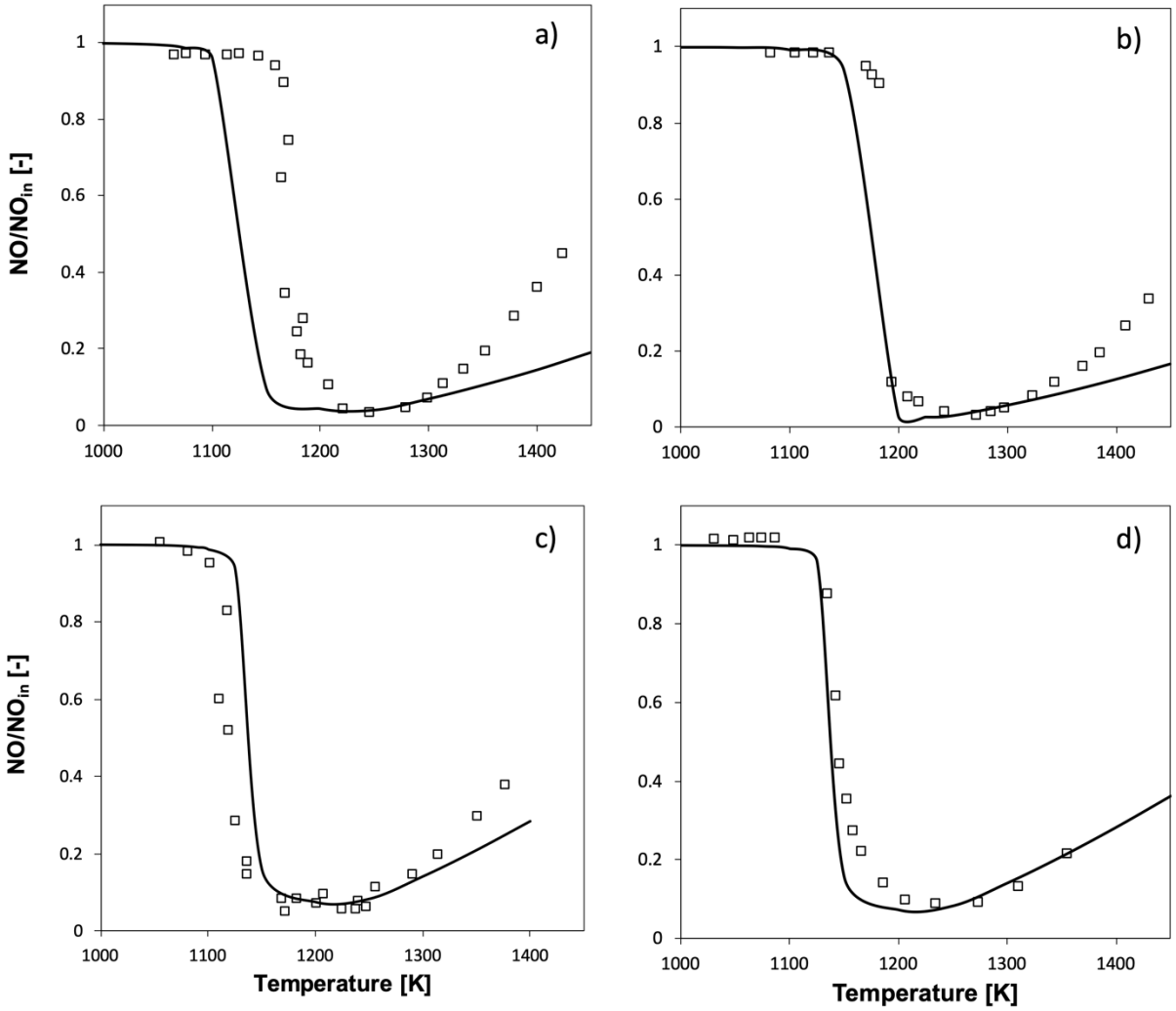

Figure S11. Oxidation of NH_3/NO mixtures with O_2 (balance gas N_2). P = 1 atm. $\tau = \frac{374}{T[K]}$ [s]. a) 7200 ppm NH_3 – 3000 ppm NO – 6% O_2; b) 7200 ppm NH_3 – 3000 ppm NO – 2% O_2; c) 1920 ppm NH_3 – 800 ppm NO – 2% O_2; d) 1920 ppm NH_3 – 800 ppm NO – 1.6% O_2.

2.2 Shock tube

2.2.1 Halat-Augier et al. [9]

Type: Shock tube

Model: Constant-volume batch reactor

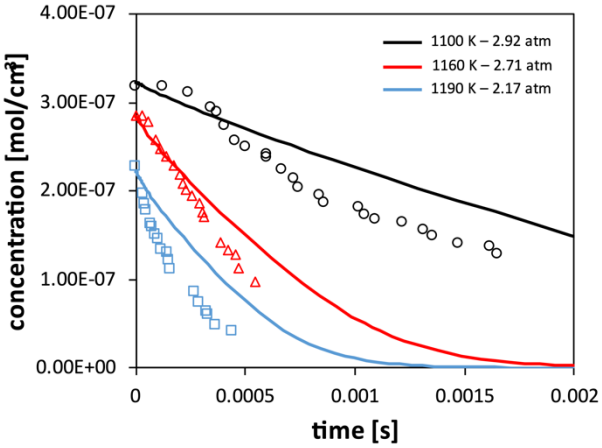

Figure S12. N_2H_4 concentration profile in the Pyrolysis of 1% N_2H_4 in N_2, observed in a shock-tube. Experimental data [9] *vs modeling results.*

2.2.2 Davidson et al. [10]

Type: Shock tube

Model: Constant-volume batch reactor

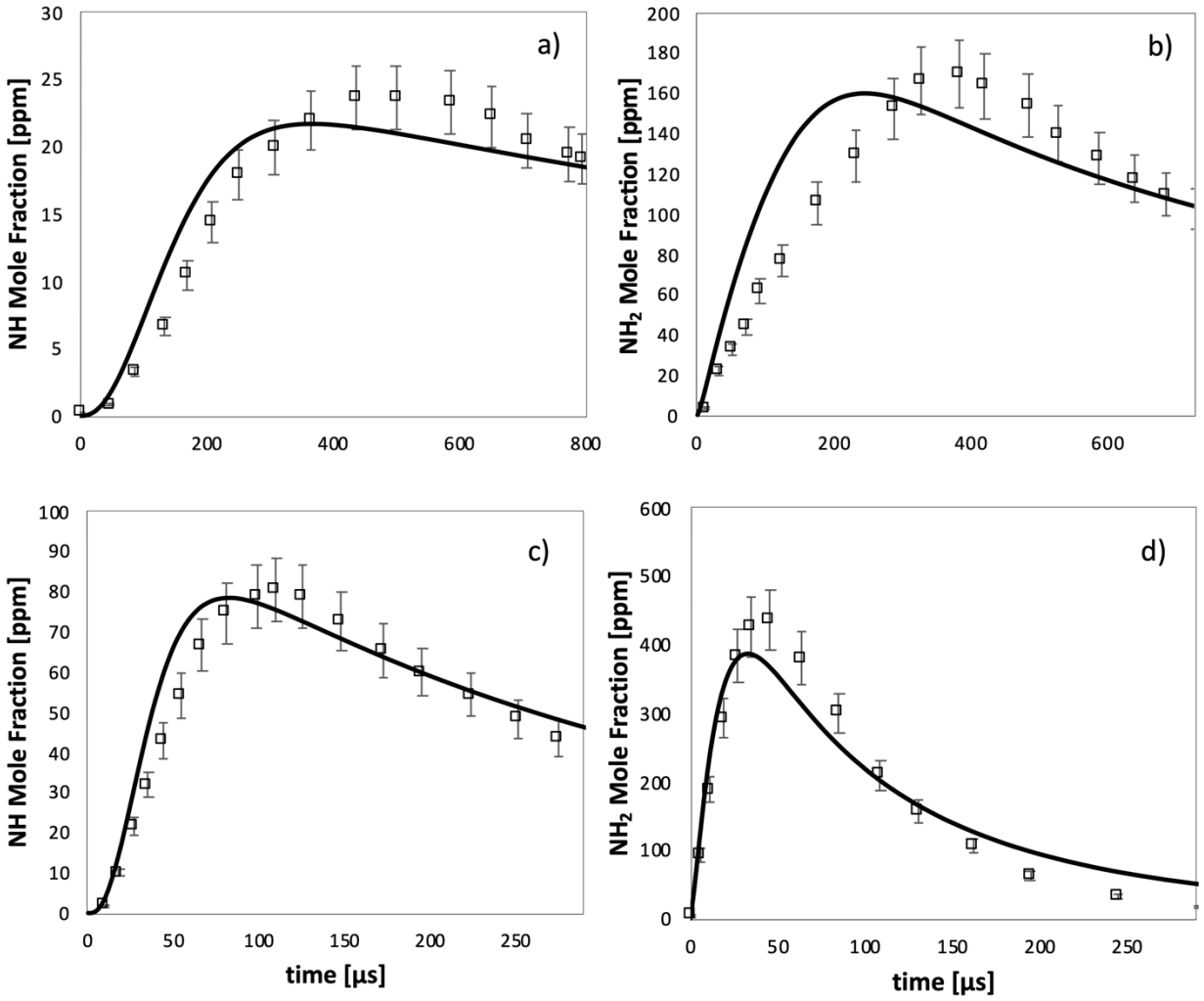

Figure S13. NH (left) and NH_2 (right) mole fractions in the pyrolysis of ammonia in a shock tube (balance gas: Ar). a) T = 2294 K – P = 0.986 atm – 3000 ppm NH_3; b) T = 2301 K – P = 1.028 atm – 2700 ppm NH_3; c) T = 2652 K – P = 0.876 atm – 3000 ppm NH_3; d) T = 2781 K – P = 0.902 atm – 2700 ppm NH_3. Experimental data [10] *vs modeling results.*

2.2.3 Mathieu and Petersen [11]

Type: Shock tube

Model: Constant-volume batch reactor

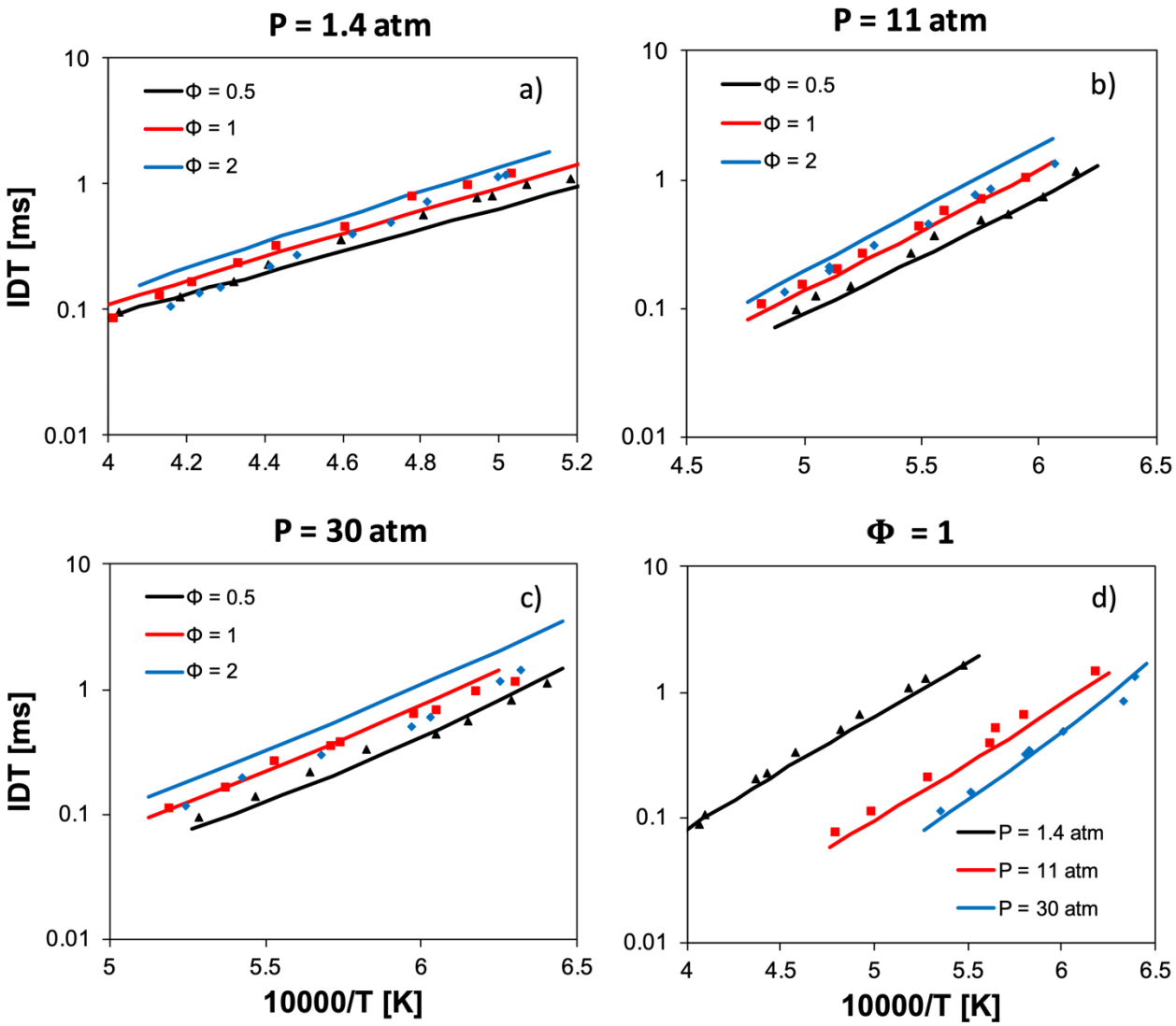

Figure S14. Ignition delay times of NH_3/O_2/Ar mixtures at variable P, Φ, dilution level. a) P = 1.4 atm – 99% Ar; b) P = 11 atm – 99% Ar; c) P = 30 atm – 99% Ar; d) Φ = 1 – 98 % Ar. Φ evaluated according to Eq. 2. Experimental data [11] *vs modeling results.*

2.2.4 Chen et al. [12]

Type: Shock tube

Model: User-defined volume batch reactor (accounting for the 2%/ms pressure rise)

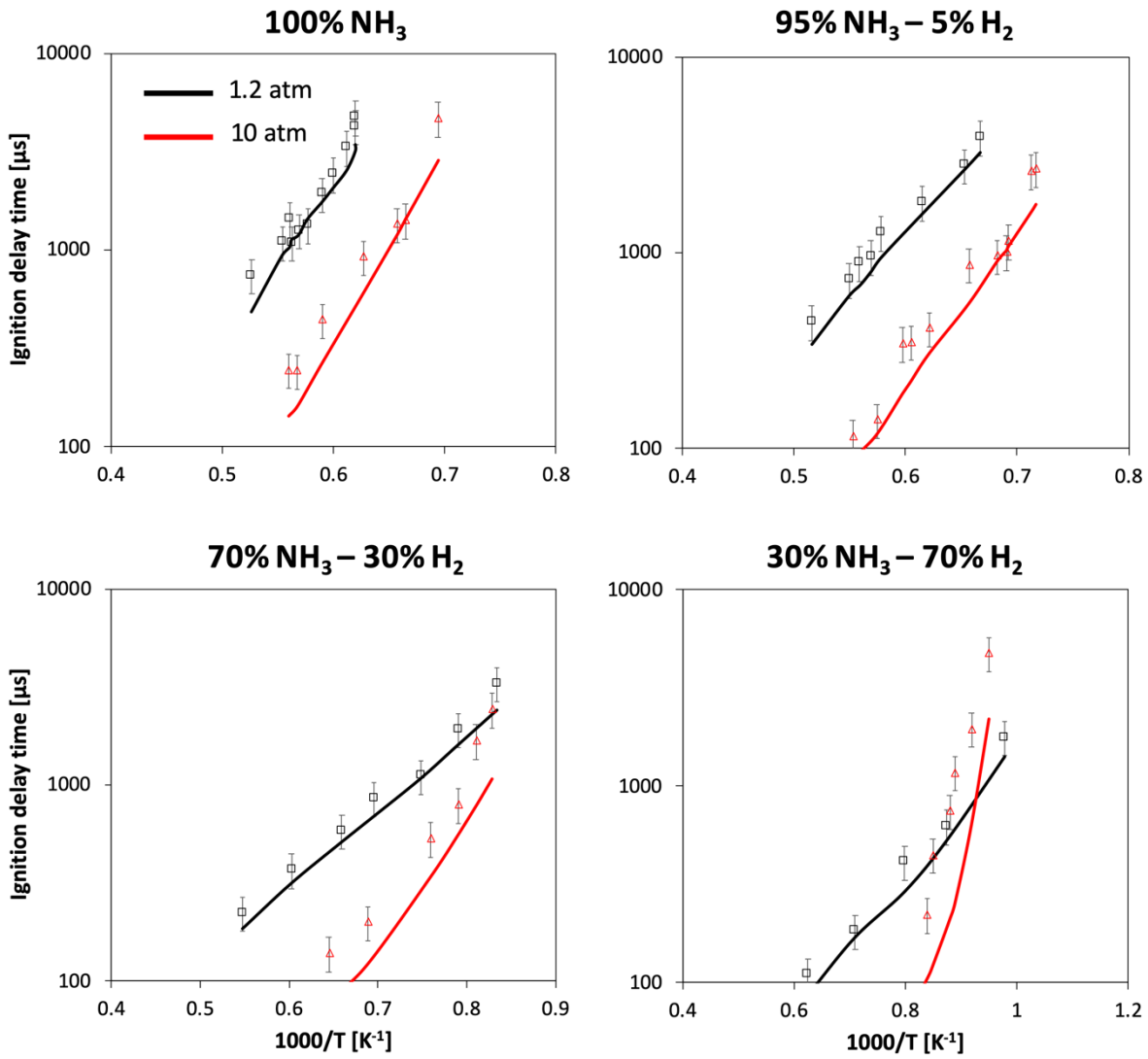

Figure S15. Ignition delay times of $NH_3/H_2/O_2/Ar$ mixtures. P = 1.2 atm, 10 atm. $\Phi = 1$. (evaluated according to Eq. 2). Detailed mixture compositions available in Table 1 of [12]. *Experimental data* [12] *vs modeling results.*

2.2.5 Shu et al. [13]

Type: Shock-tube

Model: Batch reactor with assigned volume profile (converted from experimental pressure trace)

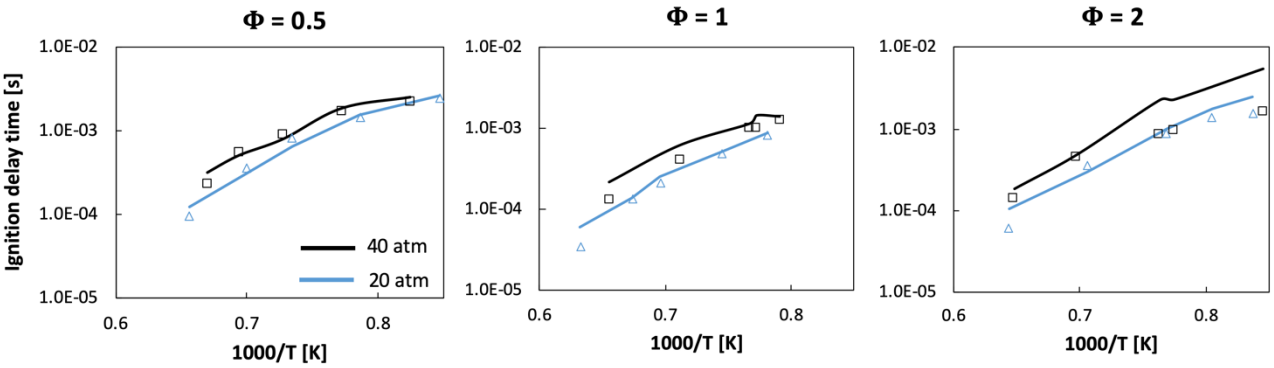

Figure S16. Ignition delay times of NH_3/air mixtures in a shock tube. P = 20, 40 atm. Experimental data [13] *vs modeling predictions. Φ evaluated according to Eq. 2.*

2.2.6 Alturaifi et al. [14]

Type: Shock tube

Model: Constant-volume batch reactor

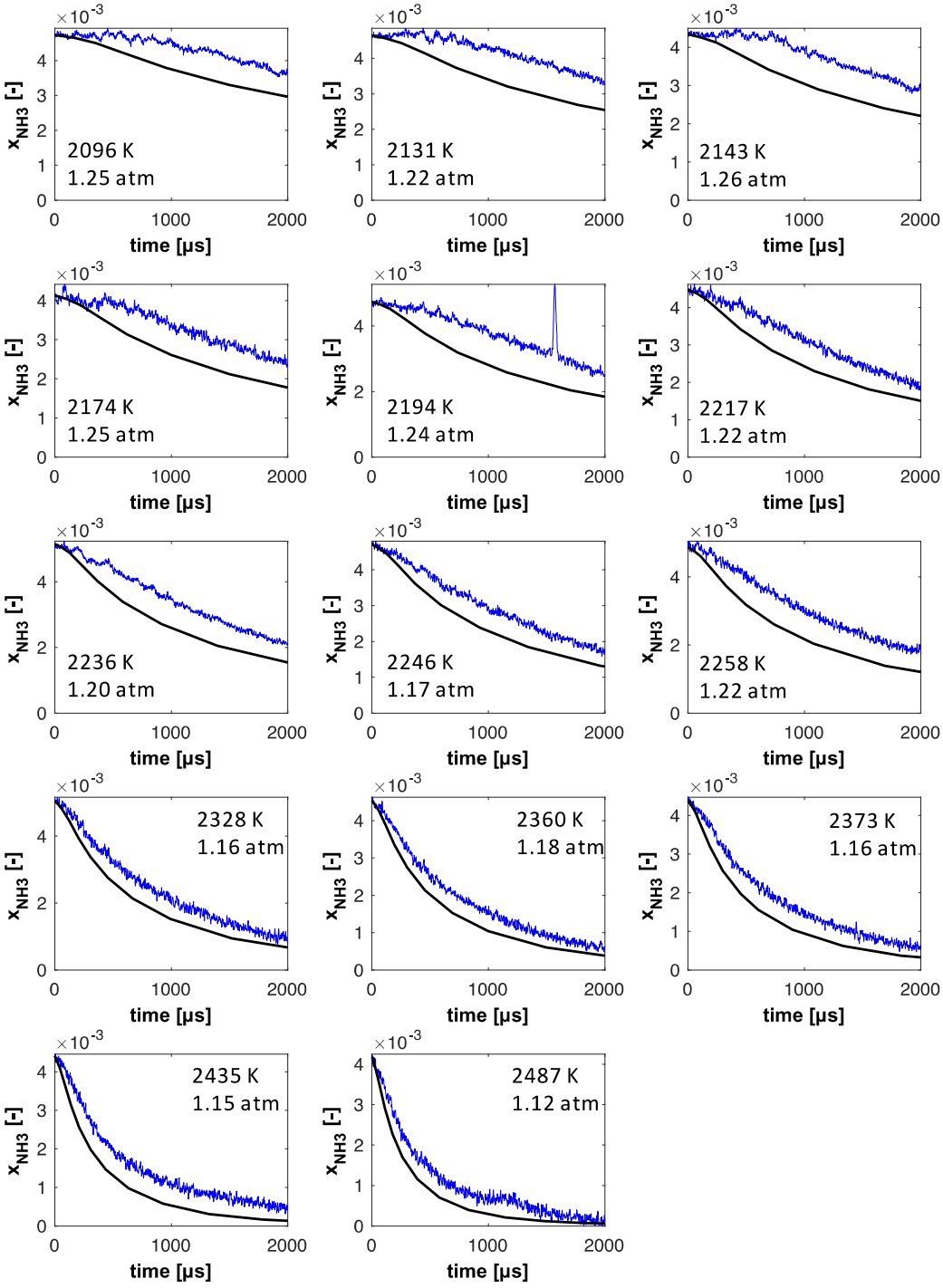

Figure S17. NH_3 speciation profiles in a mixture of ~0.5% NH_3 in Ar. Experimental data (blue lines) vs modeling predictions (black lines). Detailed compositions available in SM of [14].

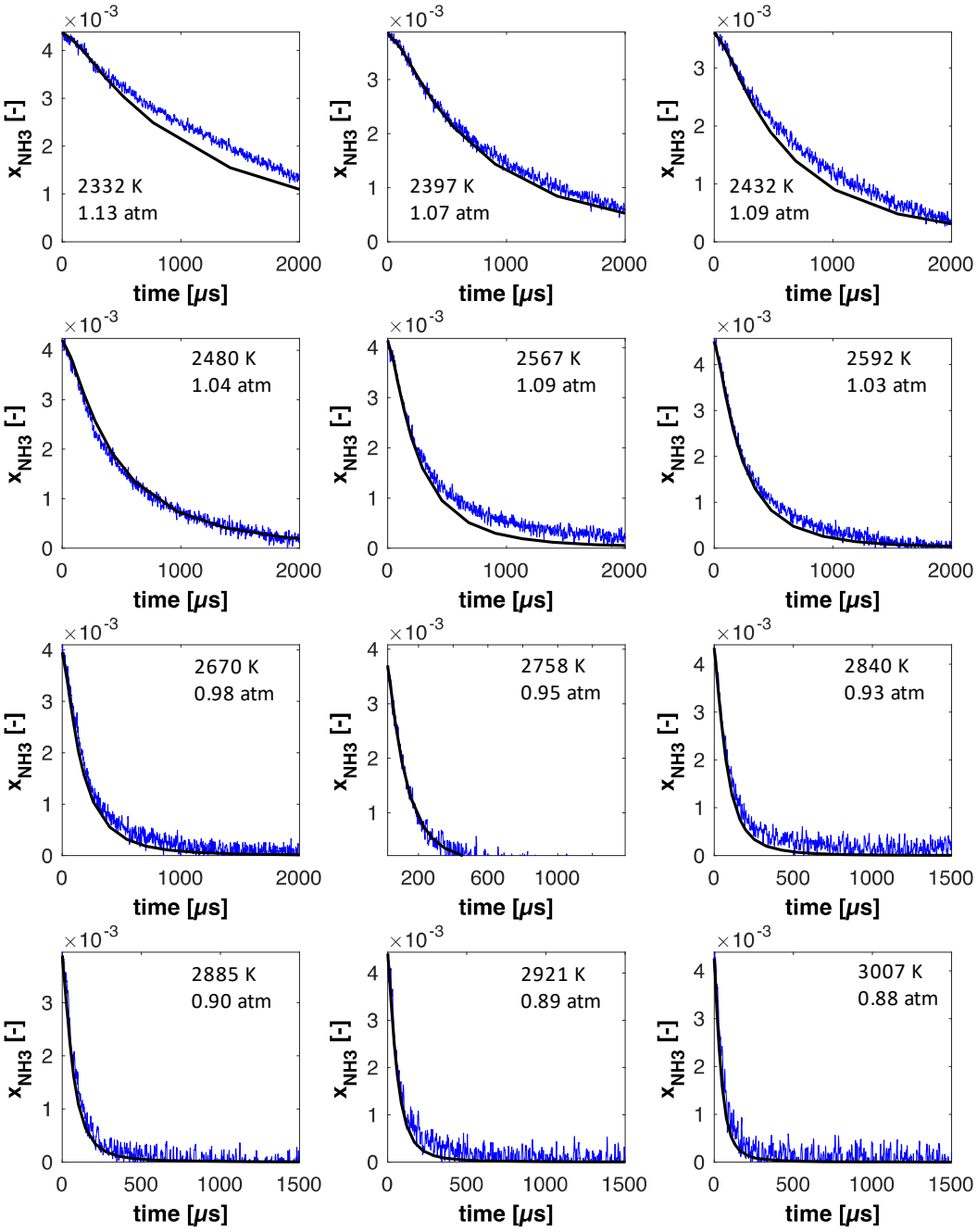

Figure S18. NH_3 speciation profiles in a mixture of ~0.42% NH_3/2% H_2 in Ar. Experimental data (blue lines) vs modeling predictions (black lines) Detailed compositions available in SM of [14].

2.2.7 Alturaifi et al. [15]

Type: Shock tube

Model: Constant-volume batch reactor

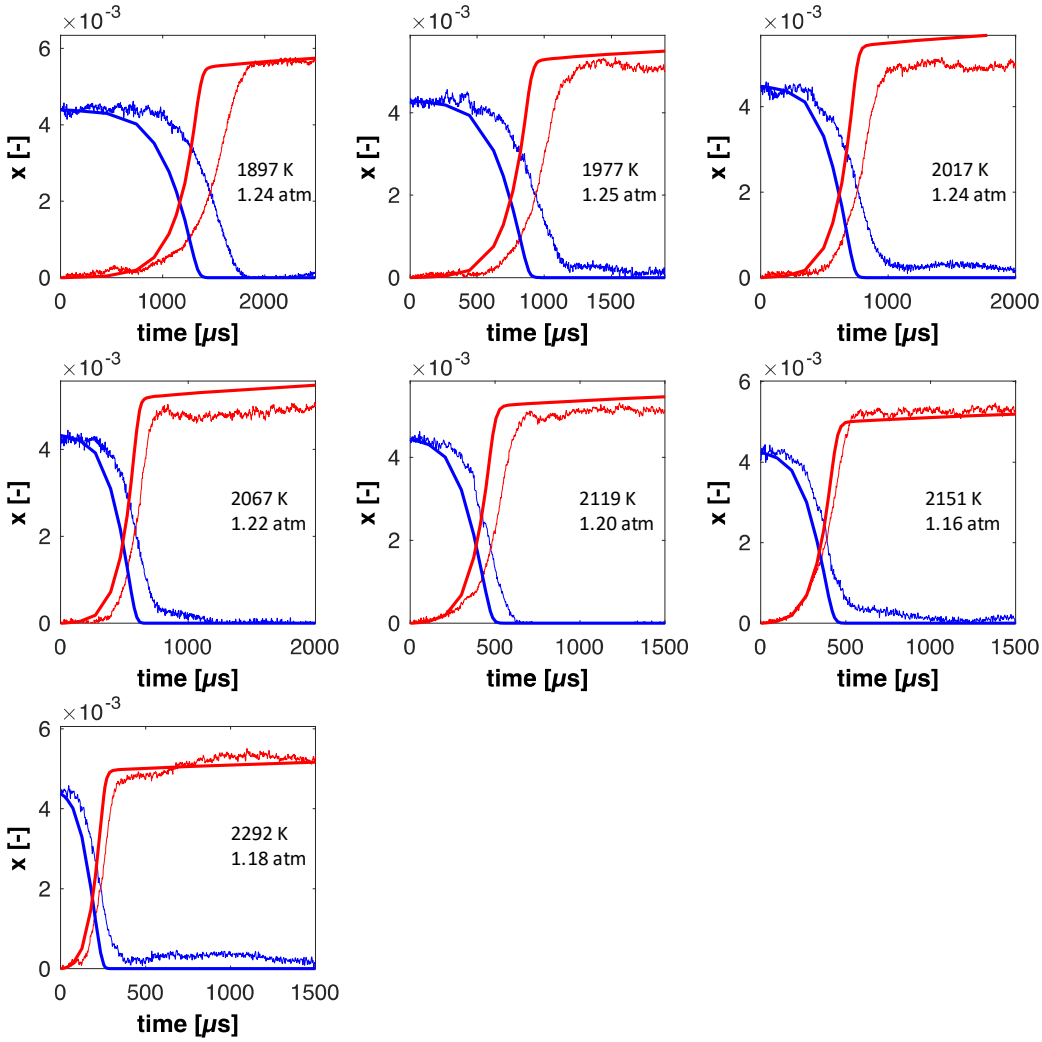

Figure S19. NH_3 (blue lines) and H_2O (red lines) speciation profiles in the oxidation of NH_3 in ~99% Ar. $\Phi_{N_2} = 0.58$. Experimental data vs modeling predictions. Detailed compositions available in SM of [15].

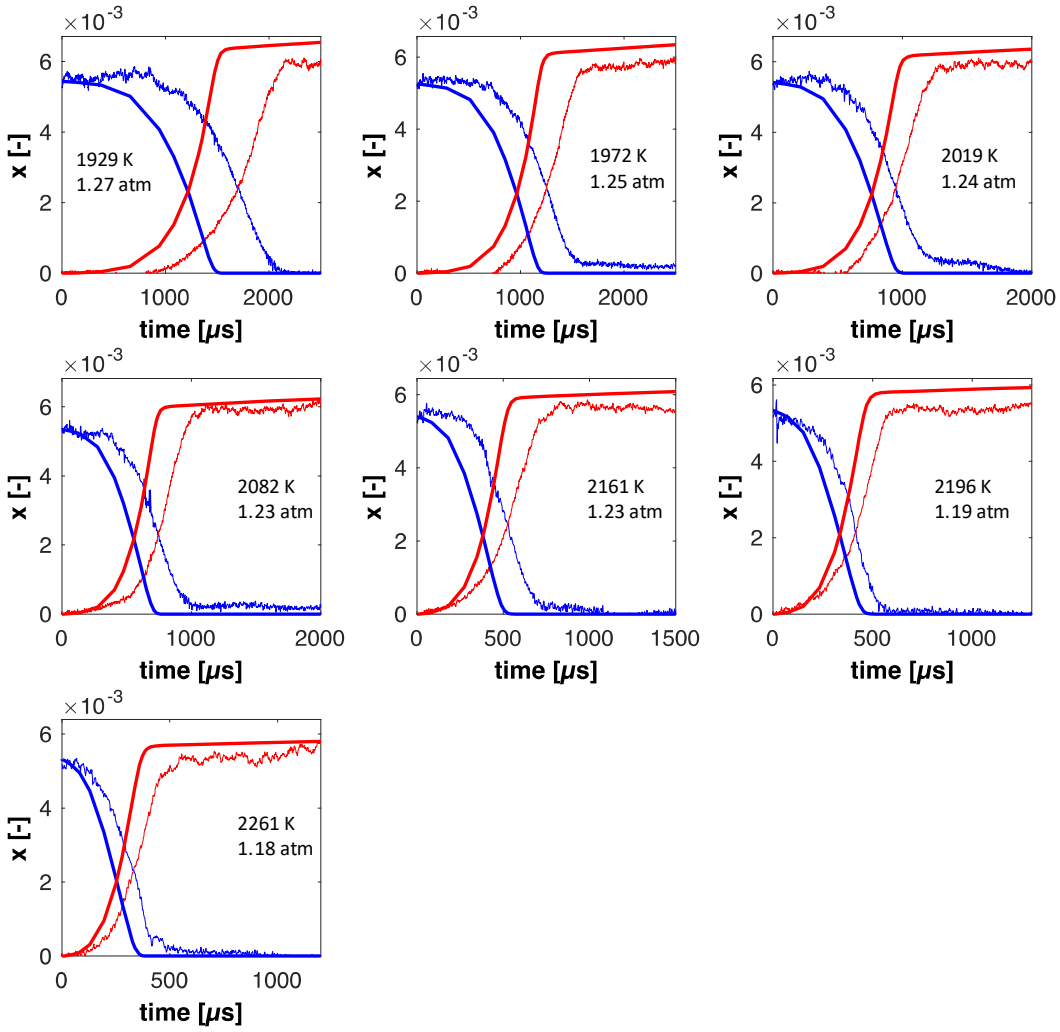

Figure S20. NH_3 (blue lines) and H_2O (red lines) speciation profiles in the oxidation of NH_3 in ~99% Ar. $\Phi_{N_2} = 0.90$. Experimental data vs modeling predictions. Detailed compositions available in SM of [15].

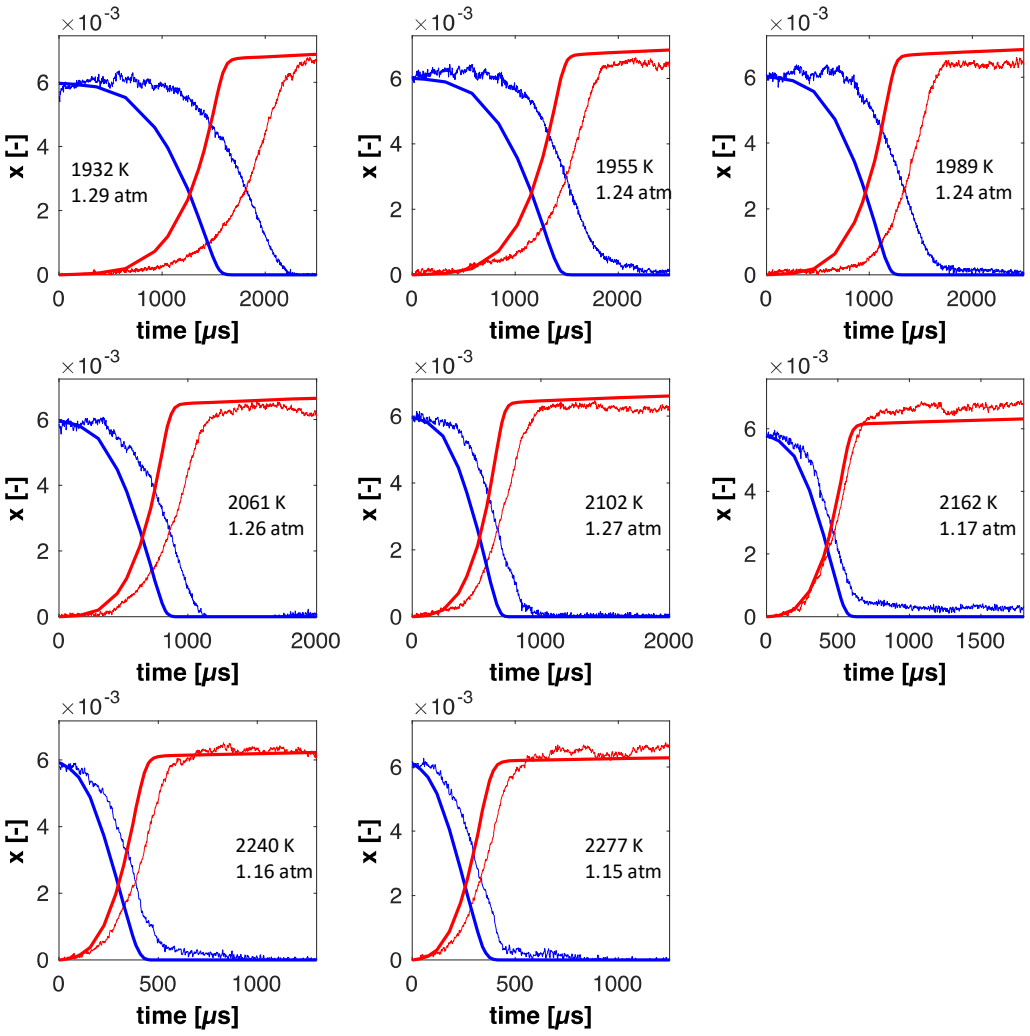

Figure S21. NH_3 (blue lines) and H_2O (red lines) speciation profiles in the oxidation of NH_3 in ~99% Ar. Φ_{N_2} = 1.06. Experimental data vs modeling predictions. Detailed compositions available in SM of [15].

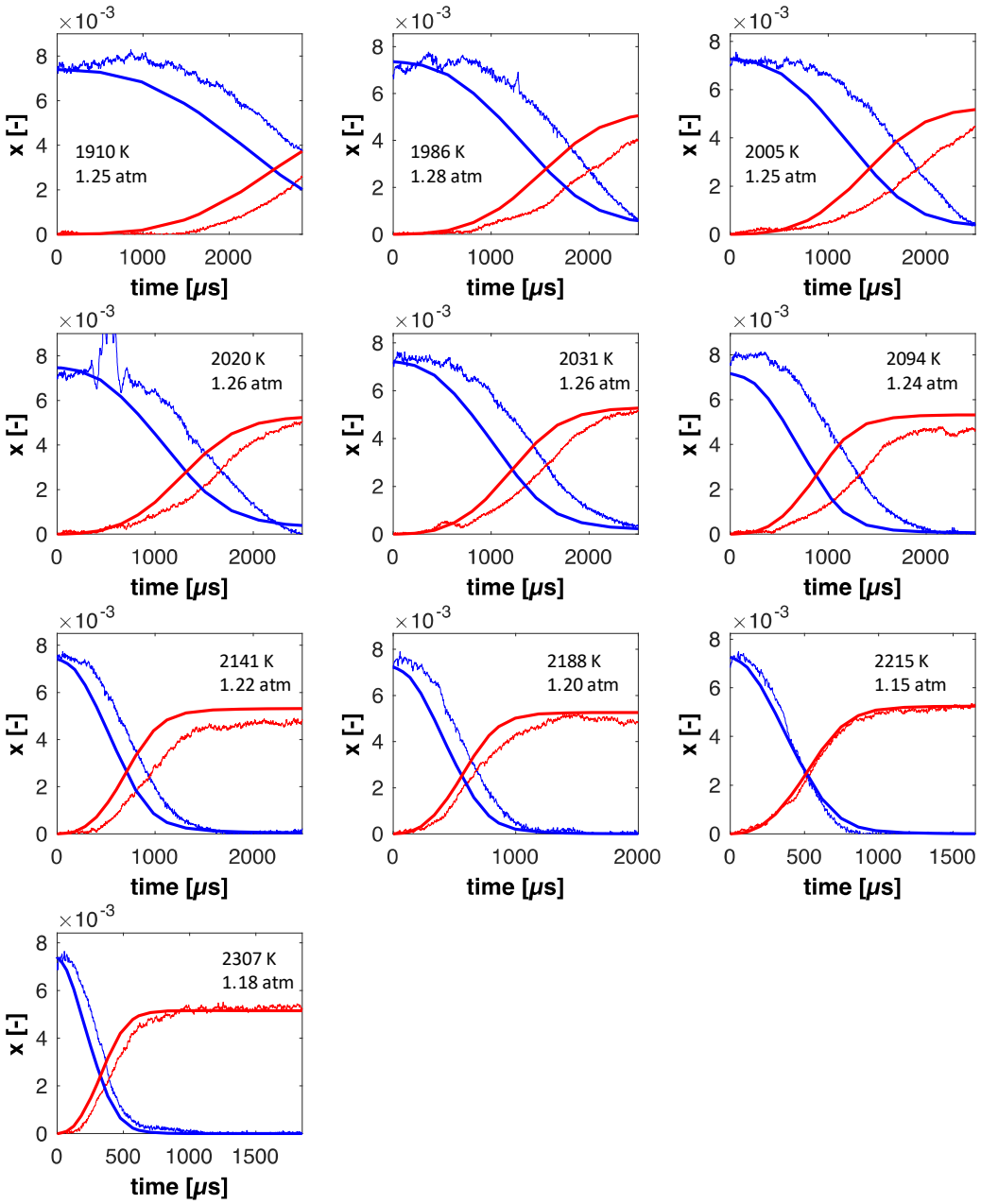

Figure S22. NH_3 (blue lines) and H_2O (red lines) speciation profiles in the oxidation of NH_3 in ~99% Ar. $\Phi_{N_2} = 2.03$. Experimental data vs modeling predictions. Detailed compositions available in SM of [15].

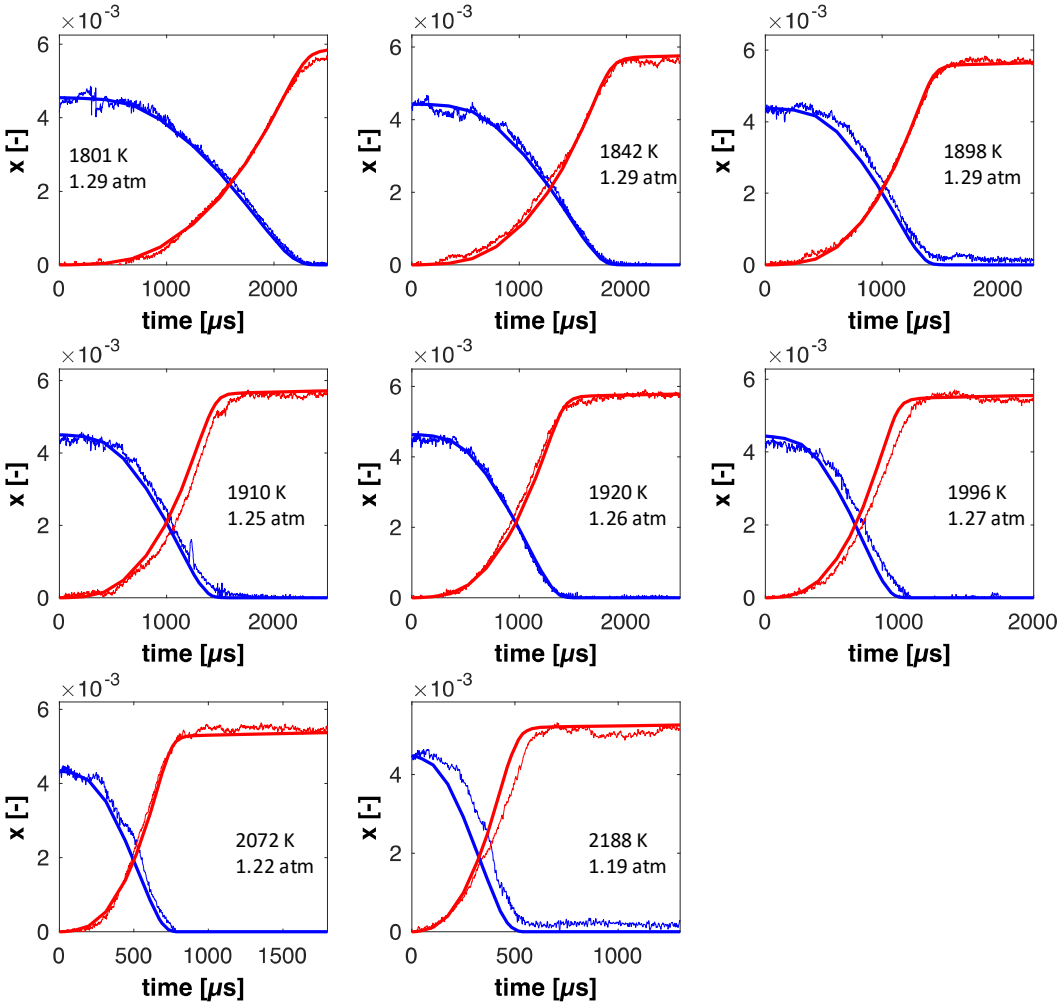

Figure S23. NH_3 (blue lines) and H_2O (red lines) speciation profiles in the oxidation of NH_3/H_2 (80:20) in ~99% Ar. Φ_{N_2} = 1.07. Experimental data vs modeling predictions. Detailed compositions available in SM of [15].

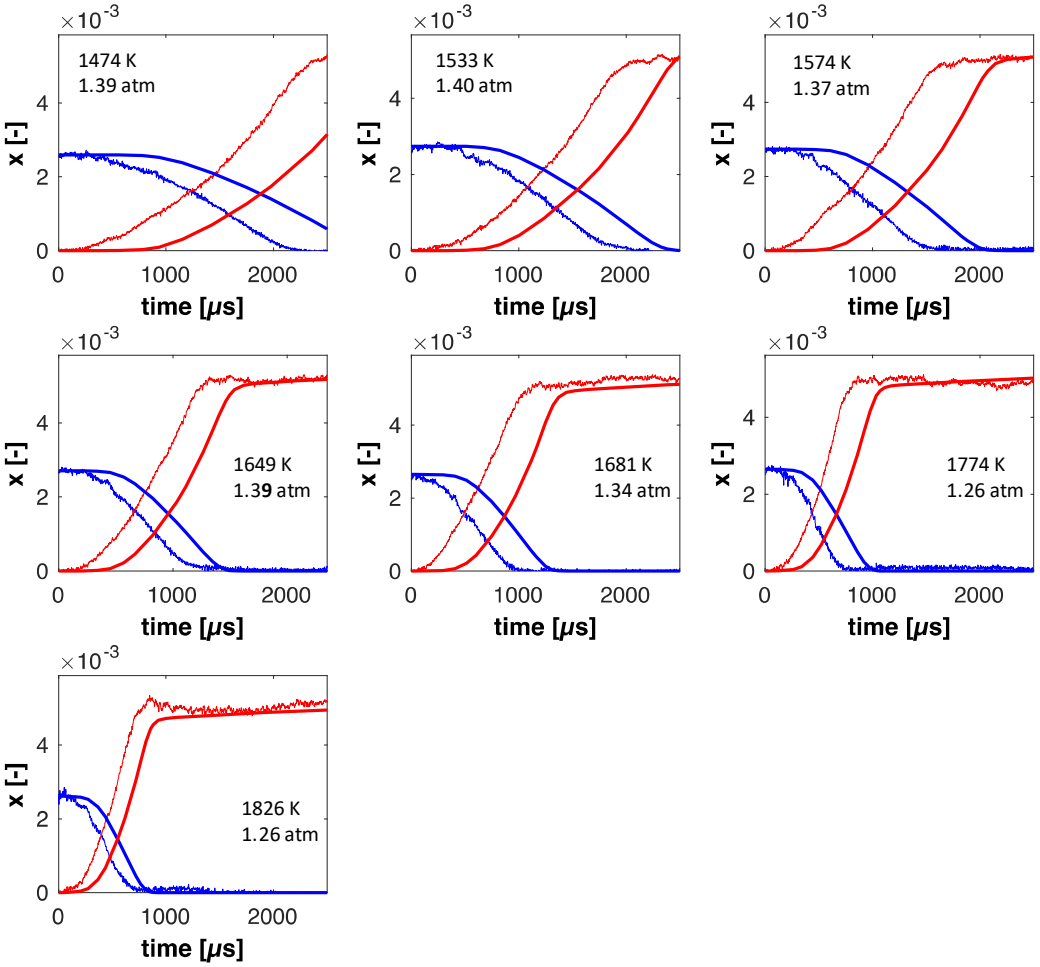

Figure S24. NH_3 (blue lines) and H_2O (red lines) speciation profiles in the oxidation of NH_3/H_2 (50:50) in ~99% Ar. Φ_{N_2} = 1.02. Experimental data vs modeling predictions. Detailed compositions available in SM of [15].

2.3 Rapid Compression Machine

2.3.1 Pochet et al. [16]

Type: Rapid compression machine

Model: Batch reactor with assigned volume profile (converted from experimental pressure trace)

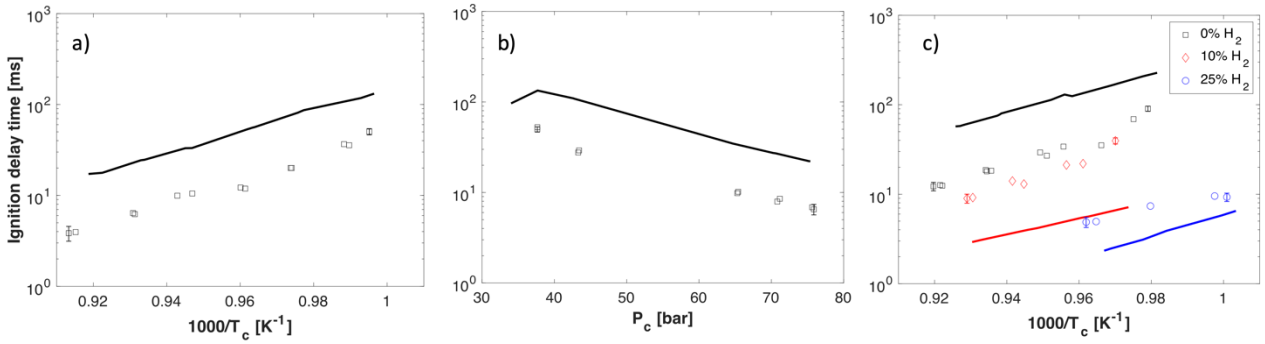

Figure S25. Ignition delay times of $NH_3/H_2/O_2/N_2/Ar$ in a rapid compression machine. Φ = 0.35 (Eq. 2). a) P_c = 65.5 bar; b) T_0 = 353 K; c) P_c = 43.4 bar. Detailed mixture compositions available in Table 2 of [16]. *Experimental data* [16] *vs modeling results.*

2.3.2 He et al. [17]

Type: Rapid compression machine

Model: Batch reactor with assigned volume profile (converted from experimental pressure trace)

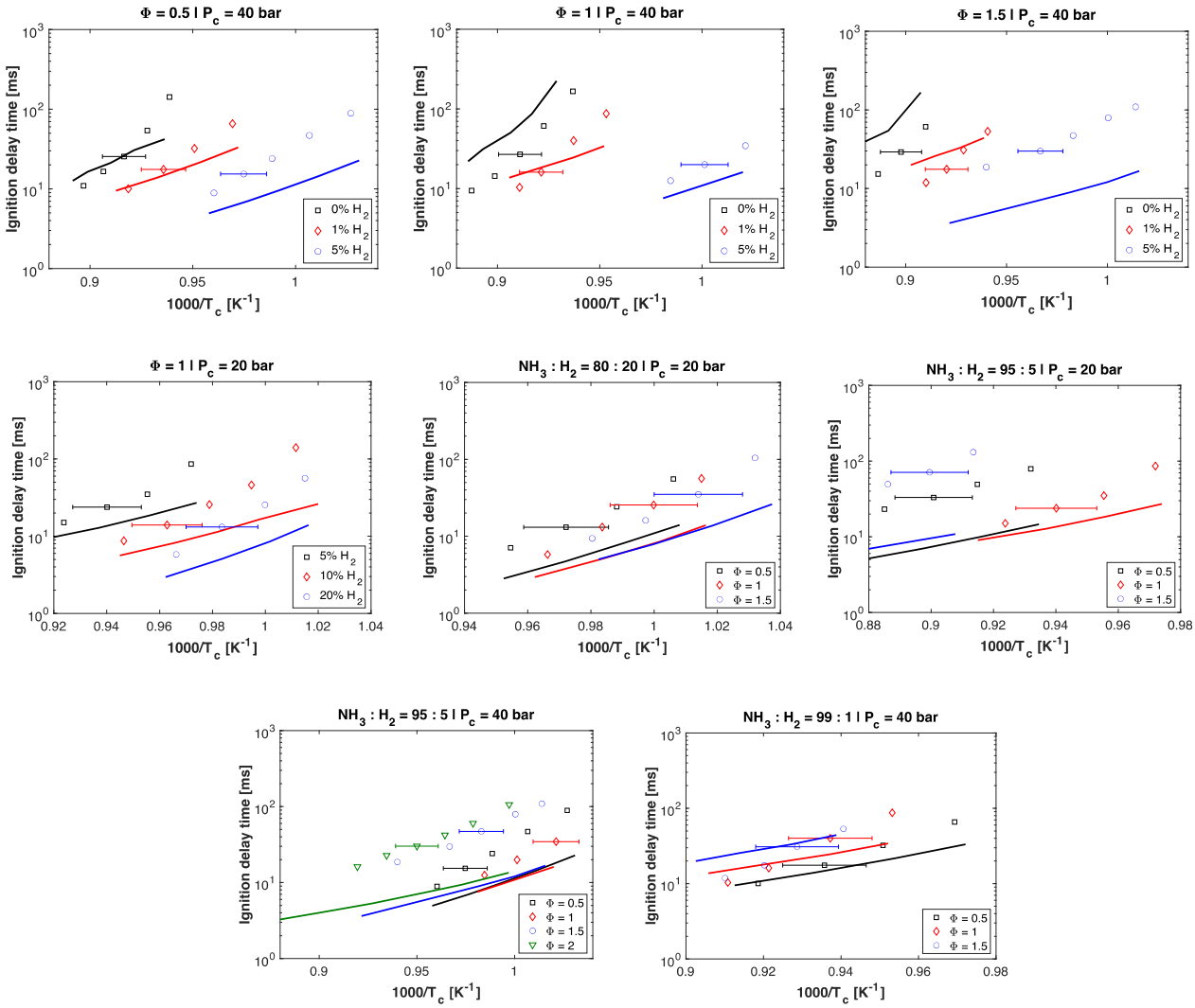

Figure S26. Ignition delay times of $NH_3/H_2/O_2/N_2/Ar$ in a rapid compression machine. (Eq. 2). Detailed mixture compositions available in Table 1 of [17]. *Experimental data* [17] *vs modeling results.*

2.4 Laminar flame speed

2.4.1 Han et al. [18]

Model: Premixed 1D laminar flame – radiation accounted for by optically-thin model

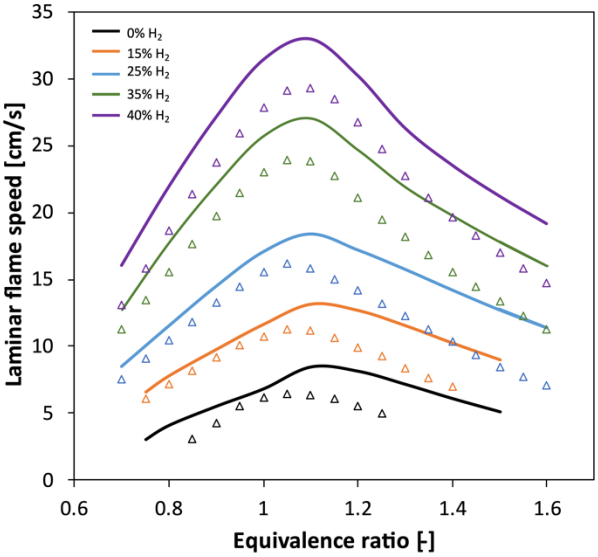

Figure S27. Laminar flame speed predictions for NH_3/H_2/air mixtures at variable pressure. T_u = 298 K. P = 1 bar. Experimental data [18] *vs modeling results.*

2.4.2 Shrestha et al. [19]

Model: Premixed 1D laminar flame – radiation accounted for by optically-thin model

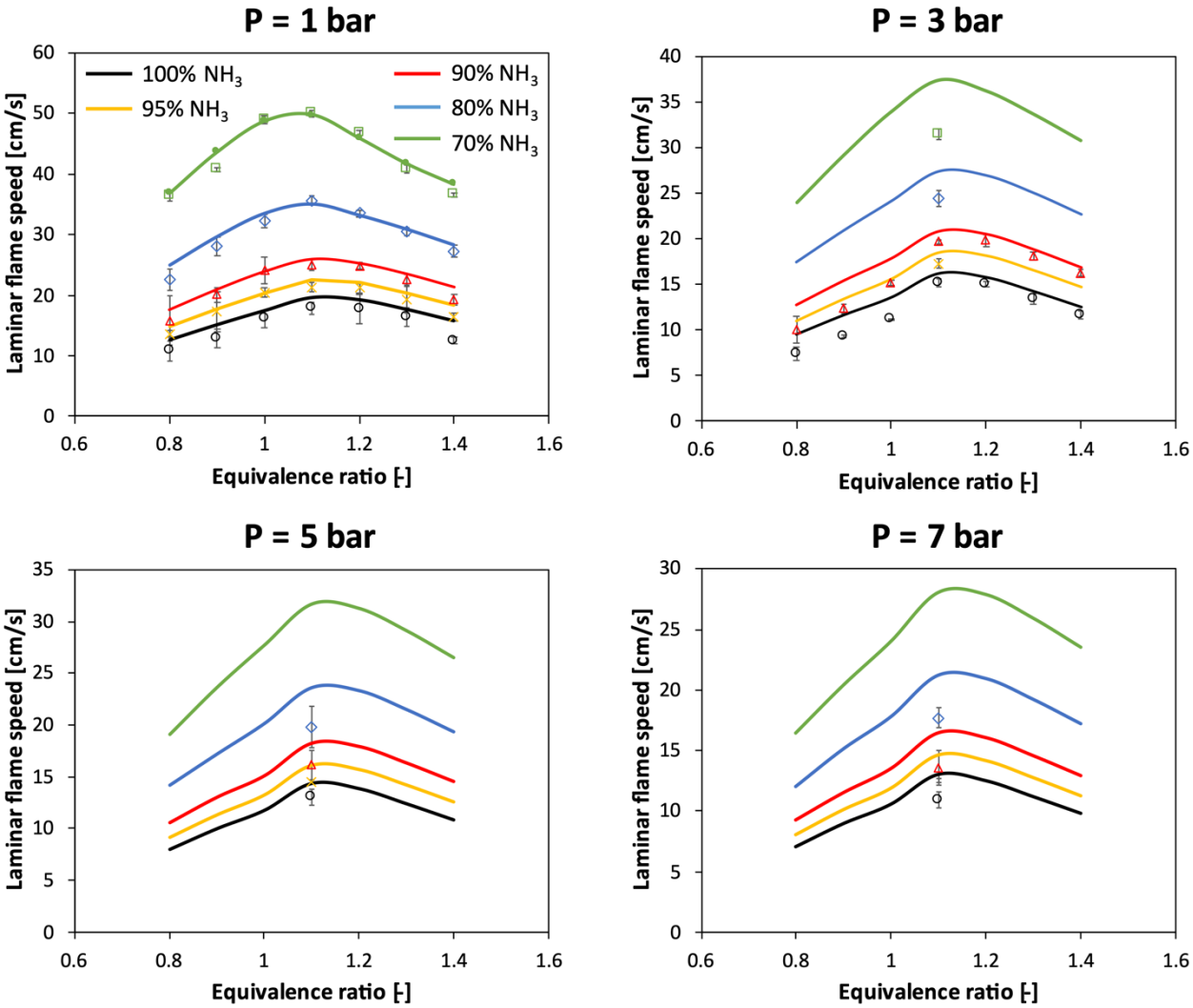

Figure S28. Laminar flame speed predictions for NH_3/H_2/air mixtures at variable pressure. T_u = 473 K. Experimental data [19] *vs modeling results.*

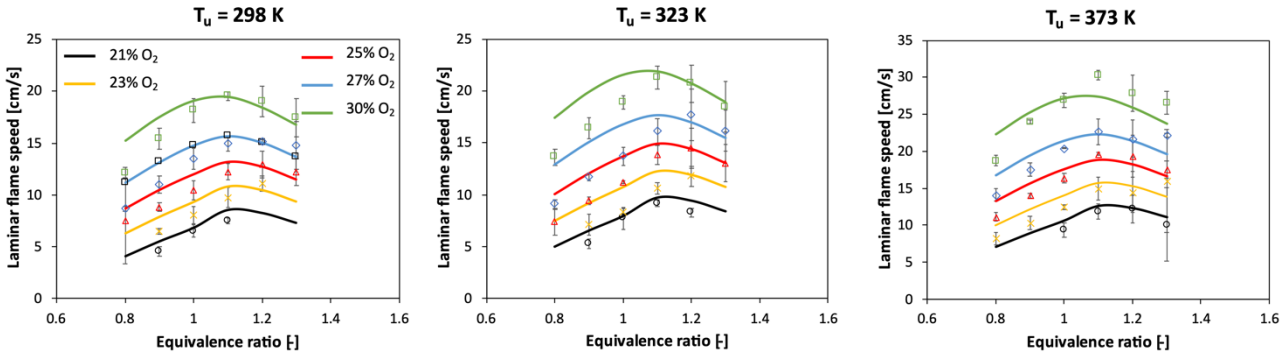

Figure S29. Laminar flame speed predictions for $NH_3/H_2/O_2/N_2$ mixtures at variable oxygen content. P = 1 bar. Experimental data [19] *vs modeling results*

2.4.3 Liu et al. [20]

Model: Premixed 1D laminar flame – radiation accounted for by optically-thin model

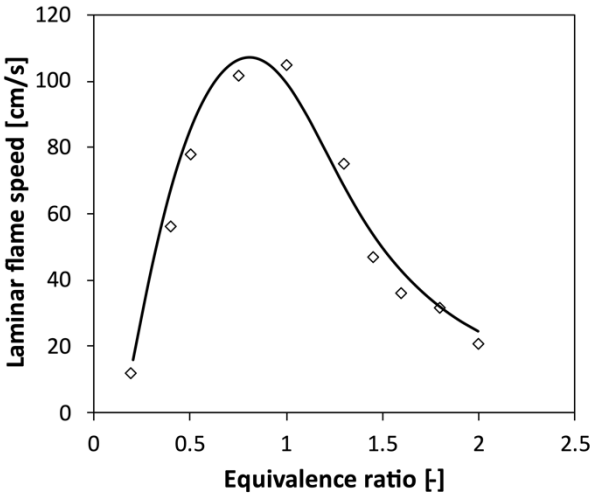

Figure S30. Laminar flame speed predictions for NH_3/O_2 mixtures at variable equivalence ratio. T_u = 298 K. P = 1 atm.

2.4.4 Mei et al. [21]

Model: Premixed 1D laminar flame – radiation accounted for by optically-thin model

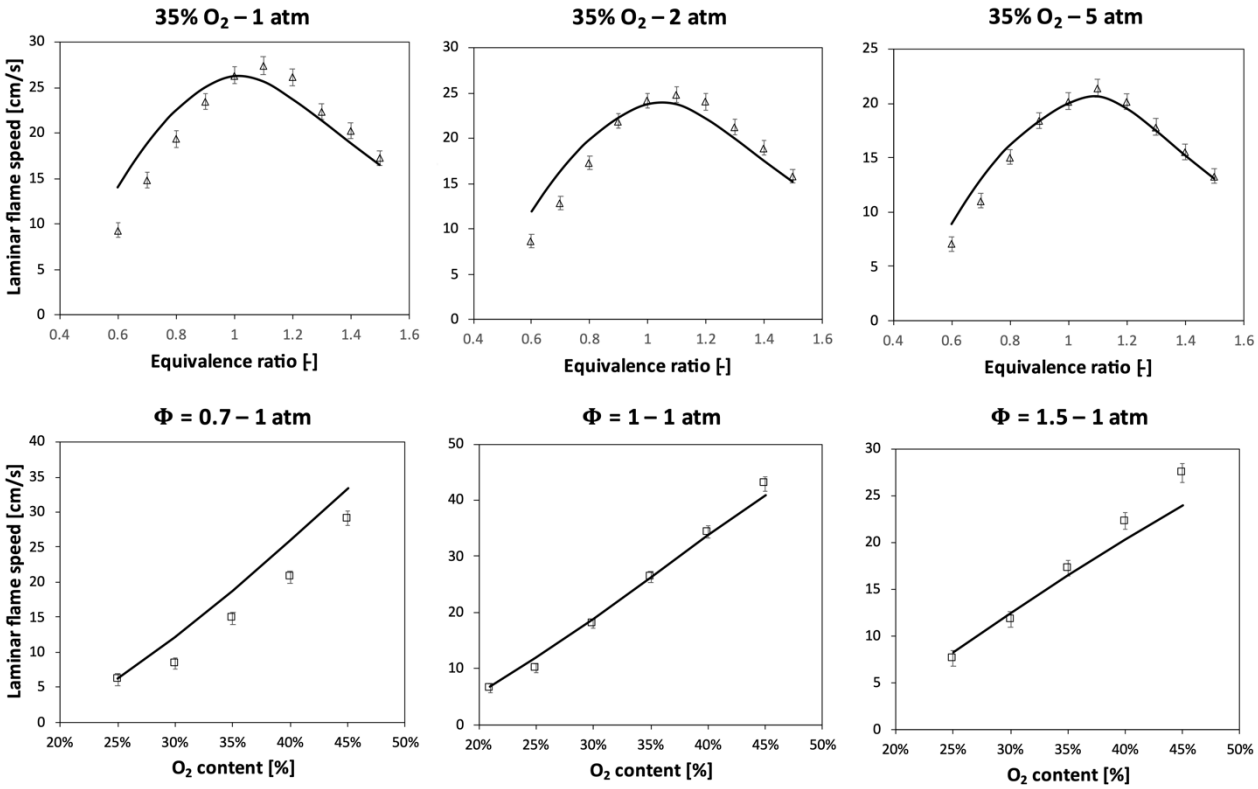

Figure S31. Laminar flame speed predictions for $NH_3/O_2/N_2$ mixtures at variable pressure and oxygen content. T_u = 298 K. Experimental data [21] *vs modeling results.*

3 References

[1] Stagni A, Cavallotti C, Arunthanayothin S, Song Y, Herbinet O, Battin-Leclerc F, et al. An experimental, theoretical and kinetic-modeling study of the gas-phase oxidation of ammonia. React Chem Eng 2020;5:696–711.

[2] Glarborg P, Miller JA, Ruscic B, Klippenstein SJ. Modeling nitrogen chemistry in combustion. Prog Energy Combust Sci 2018;67:31–68.

[3] Mei B, Zhang J, Shi X, Xi Z, Li Y. Enhancement of ammonia combustion with partial fuel cracking strategy: Laminar flame propagation and kinetic modeling investigation of NH3/H2/N2/air mixtures up to 10 atm. Combust Flame 2021;231:111472.

[4] Shrestha KP, Seidel L, Zeuch T, Mauss F. Detailed Kinetic Mechanism for the Oxidation of Ammonia Including the Formation and Reduction of Nitrogen Oxides. Energy and Fuels 2018;32:10202–17.

[5] Zhang X, Moosakutty SP, Rajan RP, Younes M, Sarathy SM. Combustion chemistry of ammonia/hydrogen mixtures: Jet-stirred reactor measurements and comprehensive kinetic modeling. Combust Flame 2021;234:111653.

[6] Sabia P, Manna MV, Ragucci R, de Joannon M. Mutual inhibition effect of hydrogen and ammonia in oxidation processes and the role of ammonia as “strong” collider in third-molecular reactions. Int J Hydrogen Energy 2020;45:32113–27.

[7] Dagaut P, Nicolle A. Experimental and kinetic modeling study of the effect of SO2 on the reduction of NO by ammonia. Proc Combust Inst 2005;30:1211–8.

[8] Rota R, Antos D, Zanoelo EF, Carrà S. Experimental study and kinetic modelling of nitric oxide reduction with ammonia. Combust Sci Technol 2001;163:25–47.

[9] Halat-Augier C, Dupre G, Paillard CE. Thermal decomposition of gaseous hydrazine behind a reflected shock wave. Proc. 20th Int. Symp. Shock waves, vol. 2, 1996, p. 893–943.

[10] Davidson DF, Kohse-Höinghaus K, Chang AY, Hanson RK. A pyrolysis mechanism for

ammonia. Int J Chem Kinet 1990;22:513–35.

[11] Mathieu O, Petersen EL. Experimental and modeling study on the high-temperature oxidation of Ammonia and related NOx chemistry. Combust Flame 2015;162:554–70.

[12] Chen J, Jiang X, Qin X, Huang Z. Effect of hydrogen blending on the high temperature auto-ignition of ammonia at elevated pressure. Fuel 2021;287:119563.

[13] Shu B, Vallabhuni SK, He X, Issayev G, Moshammer K, Farooq A, et al. A shock tube and modeling study on the autoignition properties of ammonia at intermediate temperatures. Proc Combust Inst 2019.

[14] Alturaifi SA, Mathieu O, Petersen EL. An experimental and modeling study of ammonia pyrolysis. Combust Flame 2022;235:111694.

[15] Alturaifi SA, Mathieu O, Petersen EL. A shock-tube study of NH3 and NH3/H2 oxidation using laser absorption of NH3 and H2O. Proc Combust Inst 2022.

[16] Pochet M, Dias V, Moreau B, Foucher F, Jeanmart H, Contino F. Experimental and numerical study, under LTC conditions, of ammonia ignition delay with and without hydrogen addition. Proc Combust Inst 2019;37:621–9.

[17] He X, Shu B, Nascimento D, Moshammer K, Costa M, Fernandes RX. Auto-ignition kinetics of ammonia and ammonia/hydrogen mixtures at intermediate temperatures and high pressures. Combust Flame 2019.

[18] Han X, Wang Z, Costa M, Sun Z, He Y, Cen K. Experimental and kinetic modeling study of laminar burning velocities of NH3/air, NH3/H2/air, NH3/CO/air and NH3/CH4/air premixed flames. Combust Flame 2019.

[19] Shrestha KP, Lhuillier C, Barbosa AA, Brequigny P, Contino F, Mounaïm-Rousselle C, et al. An experimental and modeling study of ammonia with enriched oxygen content and ammonia/hydrogen laminar flame speed at elevated pressure and temperature. Proc Combust Inst 2021;38:2163–74.

[20] Liu Q, Chen X, Huang J, Shen Y, Zhang Y, Liu Z. The characteristics of flame propagation in ammonia/oxygen mixtures. J Hazard Mater 2019;363:187–96.

[21] Mei B, Zhang X, Ma S, Cui M, Guo H, Cao Z, et al. Experimental and kinetic modeling investigation on the laminar flame propagation of ammonia under oxygen enrichment and elevated pressure conditions. Combust Flame 2019;210:236–46.